Experimental Measurement of Heat Collection Element Thermal Resistance for Concentrating Parabolic Solar Troughs

Anthony M. Messina[1], Rebecca L. Gardner[1], John W. Goljenboom, Jr.[1],
John D. LaFavor[1], Benjamin M. Peterson[1], and Matthew J. Traum[2]
Milwaukee School of Engineering, Milwaukee, WI, 53202

Heat Collection Elements (HCE's) mounted in the focal line of parabolic troughs are a common solution for sunlight energy capture in concentrated solar power (CSP) systems. The typical HCE is a composite device consisting of a steel pipe mounted inside an evacuated glass tube. The inner pipe is covered with a high-absorptivity coating that encourages retention of incident concentrated sunlight. The tube's vacuum must typically be maintained below the Knudsen conduction limit to mitigate thermal convection and convection losses between the inner pipe and outer glass tube. We tested an HCE 1921 mm long with a 35-mm-diameter coated steel pipe receiver mounted inside a 100-mm-diameter borosilicate glass envelope. In our static tests, heated working fluid (water) filled the HCE. An array of thermocouples mounted inside the tube measured the fluid spatial temperature profile as a function of time while the HCE was exposed to a constant temperature ambient environment. These static tests evaluated the HCE's heat transfer performance by experimentally measuring the thermal resistance it provided. Results from the static tests inform design improvements for an experimental parabolic solar trough simulator.

Nomenclature

$A_{s,O}$	=	outer surface area of the steel tube [m^2]
α	=	thermal diffusivity [m^2/s]
β	=	thermal expansion coefficient [1/K]
C_{sys}	=	thermal mass of the system [kJ/kg]
D	=	outer diameter of glass envelope [m]
ε_s	=	steel pipe coating emissivity
ε_G	=	glass envelope emissivity
$F_{0\rightarrow\lambda}$	=	radiation band emission fraction from 0 nm to λ nm
F_{12}	=	view factor between components 1 and 2
Gr	=	Grashof number
h	=	convective heat transfer coefficient [W/m^2-K]
k_{air}	=	air thermal conductivity [W/m-K]
k_{eff}	=	effective thermal conductivity [W/m-K]
k_G	=	glass thermal conductivity [W/m-k]
k_s	=	steel thermal conductivity [W/m-K]
k_w	=	water thermal conductivity [W/m-K]
L	=	heat collector element length [m]
L_c	=	characteristic length [m]
λ	=	electromagnetic radiation wavelength [nm]
Nu_D	=	Nusselt number (based on diameter)
Pr	=	Prandtl number
$R_{s,I}$	=	steel tube inner radius [m]
$R_{s,O}$	=	steel tube outer radius [m]

[1] Undergraduate Research Assistant, Mechanical Eng. Department, 1025 N. Broadway, AIAA Student Member.
[2] Assistant Professor, Mechanical Eng. Department, 1025 N. Broadway, AIAA Member.

R_1 = resistance to heat transfer via conduction through the steel tube [K/W]
R_2 = resistance to heat transfer via radiation from the steel tube to ambient [K/W]
R_3 = resistance to heat transfer via convection from the steel tube to the glass envelope [K/W]
R_4 = resistance to heat transfer via radiation from the steel tube to the glass envelope [k/W]
R_5 = resistance to heat transfer via conduction through the glass envelope [K/W]
R_6 = resistance to heat transfer from the glass envelope to ambient via natural convection [K/W]
R_7 = resistance to heat transfer via radiation from the glass envelope to ambient [K/W]
R_{eq} = total model equivalent resistance to heat transfer [K/W]
$R_{G,I}$ = glass envelope inner radius [m]
$R_{G,O}$ = glass envelope outer radius [m]
R_{tot} = total experimental resistance to heat transfer [K/W]
R_W = resistance to heat transfer via conduction through water [K/W]
Ra = Rayleigh number
Re_D = Reynolds number (based on diameter)
σ = Stefan-Boltzmann constant [W/m^2-K^4]
T = Temperature [K]
T_a = temperature of ambient air [K]
$T_{s,1}$ = temperature of inside steel tube surface [K]
$T_{s,2}$ = temperature of outside steel surface [K]
$T_{s,3}$ = temperature of inside glass envelope surface [K]
$T_{s,4}$ = temperature of outside glass envelope surface [K]
t = time [s]
υ = kinematic viscosity [m^2/s]

I. Introduction and Background

Heat Collection Elements (HCE's) mounted in the focal line of parabolic troughs are a common solution for sunlight energy capture in concentrated solar power (CSP) systems. By sizing down CSP from utility-scale plants to distributed-power-scale installations, solar-fired energy systems are now being created that are economically competitive with conventional photovoltaic (PV) arrays in the commercial- and light-industrial-building distributed power markets. Unlike conventional PV, small CSP systems can also provide combined heat-and-power (CHP) or simple heating for buildings. With only four to sixteen collection troughs, usually arranged in roof-mounted arrays, small CSP systems are much more sensitive to the performance of individual HCE's than are utility-scale CSP plants. To enable detailed parabolic trough and HCE evaluation, an apparatus was designed and built to measure key performance metrics and to evaluate system parameters in a controlled manner while closely mimicking real distributed-power-scale systems. Here we describe an experimental technique to measure total HCE thermal resistance to quantitatively evaluate how well input energy is retained by the HCE over time.

Figure 1. Performance of parabolic solar collector troughs was mimicked by a well-insulated simulator.

Previously, an array of eight sun-tracking reflective parabolic troughs supporting HCE's was designed and built (Figure 1) as the boiler for testing a novel 10 kW_e solar-fired organic Rankine cycle power plant. Since the collector array was subject to uncontrollable energy capture fluctuations due to the sun's normal diurnal motion and varying daily weather patterns, it was quickly realized that a more constant and controllable boiler was needed for power cycle testing.[1] A solar trough simulator, shown in Figure 1, was therefore constructed. The geometry of the working-

fluid-carrying tubes was matched as closely as possible between the real array and the simulator. Current-carrying thermal tape wrapped around the simulator tubes heated the working fluid and these heater-wrapped tubes were enclosed in insulating fiberglass shrouds to approximate the insulation provided by the evacuated HCE glass envelopes on the real array.

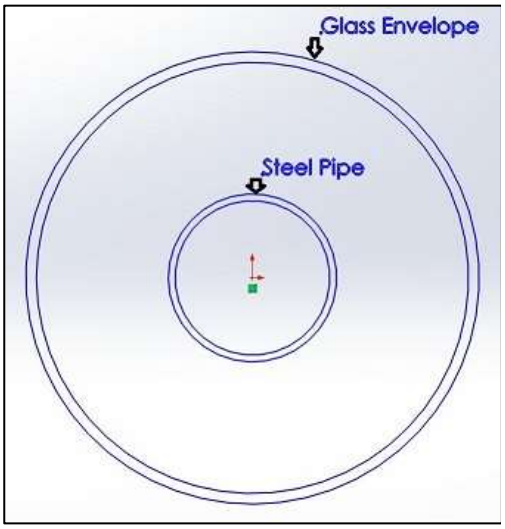

Figure 2. Heat Collection Element Cross Section

The simulator provided constant, controllable working fluid heating on-demand for testing purposes. However, it was also desirable to match the simulator's operation as closely as possible to the performance of real HCE's in parabolic troughs. A key question was whether the insulating material shrouding the simulator was providing radial resistance to heat transfer equivalent to the resistance provided by the HCE's. So, an experimental technique was developed to measure the thermal resistance provided by HCE's. This experimental technique was validated using a heat transfer model based on an equivalent thermal resistance analysis.

Each HCE is made from a 304 stainless steel pipe mounted inside an evacuated borosilicate glass envelope; see the schematic in Figure 2. The glass permits sunlight to enter and strike the tube, which is covered by a Schott coating[2] that has a high sunlight absorptivity of approximately 95% while presenting a low irradiative emissivity of approximately 10%. A vacuum is maintained in the annular space between the steel tube and the glass envelope to mitigate thermal losses via conduction or natural convection. Minimizing heat loss is desirable because the tube typically carries working fluid, which is heated by the sun, undergoing an evaporative phase change. The resulting vapor is usually then sent to a turbine to generate mechanical power to produce electricity.

Borosilicate glass is preferred for the envelope owing to its favorable optical properties and low coefficient of thermal expansion. Borosilicate glass transmits 96% of incident electromagnetic radiation from approximately 200 to 3000 nanometers wavelength, meaning it is nearly perfectly transparent to visible light. At wavelengths between 3000 and 5000 nanometers the electromagnet transmissivity drops significantly, and at wavelengths above 5000 nanometers borosilicate glass is opaque.

II. Theoretical Heat Transfer Model

Bialobrzeski provides a complete thermal resistance network for a solar HCE and describes how each equivalent resistance is calculated.[3] We applied this model for heat transfer analysis, but we added an additional resistor, R_2, which accounts for direct irradiative heat transfer from the enclosed steel tube surface to the ambient environment over the portion of electromagnetic spectral wavelengths where borosilicate is transparent. This resistance is very large when the steel receiver tube is between 300 K and 400 K (as it was in our experiments) since the fraction of radiation transmitted at longer wavelengths associated with low temperature is essentially nil. However, in actual HCE operation, especially when the working fluid is superheated, the steel tube can reach temperatures where a non-trivial fraction of its radiated energy is in the visible spectrum, and R_2 cannot be ignored. Recognizing this additional heat transfer path represents an important improvement to the standard HCE thermal performance model.

The heat transfer resistance network used in our analysis is shown in Figure 3. We assume one-dimensional heat transfer radially outward from the steel tube through the evacuated annulus and the glass envelope to ambient. Each element is assumed to be isothermal. Temperature data were recorded at six equally-spaced azimuthal locations at the geometric center and at a quarter of the axial length down the HCE analyzed. Azimuthal profiles showed uniform temperature within experimental uncertainty, validating the isothermal assumption. Moreover, the axial equivalent thermal resistance presented by half the heat collection element is estimated at 87.34 K/W while the radial resistance is about 0.64 K/W. This two-orders-of-magnitude difference between axial and radial heat transfer resistances coupled with experimental results indicating no measureable temperature

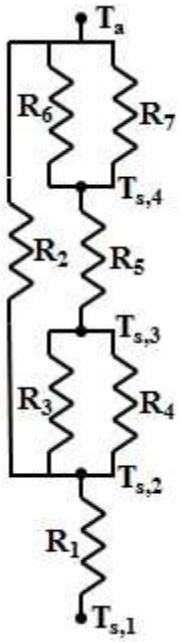

Figure 3. Heat Transfer Resistance Network.

difference between the steel pipe wall at the HCE's center versus at a quarter of its length validate the one-dimensional resistance modeling assumption.

Here we briefly describe what physical heat transfer process each resistor in the network represents and how each resistance value is evaluated.

A. Resistor One (R_1): Conduction Through the Steel Tube

R_1 is modeled using conduction in cylindrical coordinates. For the experiments herein, the steel tube was filled with stationary hot water, which (as will be shown later) behaved as a lumped capacitance. Thus, both the water temperature and tube inner wall temperature were at $T_{s,1}$. Properties for 304 stainless steel were evaluated at 400 K.

$$R_1 = \frac{ln\left(\frac{R_{S,O}}{R_{S,I}}\right)}{2\pi k_S L} \quad \text{(Eq. 1)}$$

B. Resistor Two (R_2): Radiation From the Steel Tube to Ambient

R_2 is modeled as a long cylinder radiating to the surroundings with a View Factor of 1. However, heat is only radiated via this mechanism at wavelengths in the electromagnetic spectrum from 200 nm to about 3000 nm where the borosilicate glass envelope transmits about 96% the energy incident upon it. Outside the 200 – 3000 nm wavelength band, borosilicate glass is opaque, and heat transfer associated with this portion of the spectrum is represented in the thermal circuit by R_4. For the experiments herein, the steel tube never exceeded 355 K, a temperature corresponding to λT products of 71 μm-K ($F_{0\rightarrow 200nm} = 0.000000$) and 1065 μm-K ($F_{0\rightarrow 3000nm} = 0.000910$) for λ = 200 nm and λ = 3000 nm respectively. The resulting thermal resistance equation follows.

$$R_2 = \frac{1}{\varepsilon_S A_{S,O} \sigma F_{1,2}\left(F_{0\rightarrow 3000nm} - F_{0\rightarrow 200nm}\right)(T_{S2}+T_a)(T_{S2}^2+T_a^2)} \quad \text{(Eq. 2)}$$

This heat transfer path cannot be ignored for HCE's operating at temperatures high enough to make $F_{0\rightarrow 3000nm}$ an appreciable fraction of 1. However, for the experiments herein $R_2 \approx 4155$ K/W, which is enormous compared with the parallel resistance path in the circuit of Figure 3. So, this heat transfer path is ignored here.

C. Resistor Three (R_3): Natural Convection in the Evacuated Annulus

The HCE annulus is evacuated to mitigate conductive and convective heat transfer losses. Nonetheless, trace gas remaining in the space may transport heat via natural convection. So, R_3 is modeled as natural convection heat transport between two long concentric cylinders. An effective gas conductance is calculated from the following correlation.[4]

$$\frac{k_{eff}}{k_{air}} = 0.386\left(\frac{Pr}{0.861+Pr}\right)^{\frac{1}{4}} Ra^{\frac{1}{4}} \quad \text{(Eq. 3)}$$

where the Rayleigh number characteristic length is given by the following equation,

$$L_c = \frac{2\left[ln\left(\frac{R_{G,I}}{R_{S,O}}\right)\right]^{\frac{4}{3}}}{\left(R_{G,I}^{-\frac{3}{5}} + R_{S,O}^{-\frac{3}{5}}\right)^{\frac{5}{3}}} \quad \text{(Eq. 4)}$$

and the Rayleigh number equation is the following.

$$Ra = \frac{g\beta(T_{S3}-T_{S4})L_c^3}{\upsilon\alpha} \quad \text{(Eq. 5)}$$

The resulting resistance for conduction across the annular gap using the modified conductance found previously in in Eq. 3. is the following

$$R_3 = \frac{ln\left(\frac{R_{G,I}}{R_{S,O}}\right)}{2\pi k_{eff} L} \quad \text{(Eq. 6)}$$

As will be described in the Discussion section, R_3 is very sensitive to the k_{air} value used. For this analysis, the rarified gas in the HCE's annular space was assumed to behave as ideal gas since its temperature and pressure were far from critical values. The thermal conductivity of ideal gas is not a function of pressure. So, the k_{air} used was for air a 1 atmosphere pressure and 325 K, the mean between the steel tube's hottest temperature and the glass envelope's temperature, both measured experimentally.

D. Resistor Four (R_4): Radiation From the Steel Tube to Glass Envelope

R_4 is modeled as radiation heat transfer between two long concentric cylinders. It is modified to account for the emissivity differences between the steel pipe and glass envelope. A view factor is normally included in the equation, but it is neglected here because the view factor between concentric cylinders is 1.

$$R_4 = \frac{\frac{1}{\varepsilon_S} + \frac{1-\varepsilon_G}{\varepsilon_G}\left(\frac{R_{G,I}}{R_{S,O}}\right)}{\sigma A_{S,O} 4\left(\frac{(T_{S2}+T_{S3})}{2}\right)^3} \quad \text{(Eq. 7)}$$

E. Resistor Five (R_5): Conduction Through the Glass Envelope

R_5 is modeled using conduction in cylindrical coordinates. Properties for borosilicate glass were evaluated at 300 K.

$$R_5 = \frac{ln\left(\frac{R_{G,O}}{R_{G,I}}\right)}{2\pi k_G L} \quad \text{(Eq. 8)}$$

F. Resistor Six (R_6): Natural Convection from the Glass Envelope Outer Surface

In the real parabolic trough solar collector system, ambient conditions (i.e., how fast the wind is blowing) determine if external heat loss occurs by forced or by free convection. To determine which convection mode is dominant, the ratio of Grashof number to the square of the Reynolds number is evaluated.

$$\frac{Gr}{Re_D^2} \quad \text{(Eq. 9)}$$

If this ratio is much less than 1, free convection is negligible and forced convection dominates. If the ratio is much greater than 1, forced convection is negligible and free convection dominates. Both free and forced convection occur simultaneously when the ratio is about 1. The experiment was run indoors where the environmental air velocity and hence the Reynolds number were zero. So, the ratio of Eq. 9 was therefore infinite, and free convection was used to evaluate R_6.

$$R_6 = \frac{1}{hA_{G,O}} \quad \text{(Eq. 10)}$$

The convection coefficient, h, is found from a Nusselt number correlation for natural convection over a heated horizontal cylinder,[4]

$$Nu_D = \frac{hD}{k} = \left\{0.60 + \frac{0.387Ra^{\frac{1}{6}}}{\left[1+(0.559/Pr)^{9/16}\right]^{8/27}}\right\}^2 \quad \text{(Eq. 11)}$$

where the Rayleigh number was determined by using Eq. 5 with L_c = D and a temperature difference between T_{s4} and T_a.

G. Resistor Seven (R_7): Radiation From the Glass Envelope to Ambient

R_7 is modeled as a long cylinder radiating to the surroundings with a view factor of 1. Emissive properties of borosilicate glass at 300 K are used. Duffie and Beckman[5] explain that the variation between sky temperature (or surrounding surface temperature in the case of experiments herein) and ambient air temperature will not

significantly alter the thermal radiation heat loss from a surface; so ambient temperature, T_a, is used, allowing R_7 to terminate at the same temperature node as other resistors in the network (see Figure 3).

$$R_7 = \frac{1}{\varepsilon_G A_{G,O} \sigma 4 \left(\frac{T_{s4}+T_a}{2}\right)^3} \quad \text{(Eq. 12)}$$

H. Equivalent Resistance (R_{eq}) for the Overall Resistor Network

The above modeling assumptions were applied to calculate values for each thermal resistance. Then the resistance network in Figure 3 was simplified into a single equivalent resistance: R_{eq} = 0.6459 K/W.

III. Experimental Description and Results

The experiment measured the temperature-time history of a HCE undergoing a cool-down from elevated temperature. The steel tube was completely filled with heated water at approximately 355 K and allowed to cool to ambient temperature, approximately 293 K. The system took approximately 17 hours to reach ambient temperature, as shown in Figure 4. Temperatures-time histories were logged from thermocouples placed on the inside surface of the steel tube and the outside surface of the glass envelope. Temperatures were measured at the center of the HCE and at one quarter of its length. Six thermocouples were distributed around the azimuth at each location. This configuration was selected to evaluate validity of the isothermal component and one-dimensional resistance model assumptions.

A. Lumped Capacitance Model

The simplest model that accurately captures the HCE cool-down process in the experiment is lumped capacitance. This model assumes that all the system's thermal mass resides in the stationary water while all resistance to heat transfer is presented by the HCE. In other words, the water supports no internal temperate gradient. This modeling assumption is valid, provided the Biot number for the water is less than 0.1. For this system, the Biot number is calculated as the ratio of heat transfer resistance internal to the water over R_{eq} from the HCE.

$$Bi = \frac{R_{water}}{R_{eq}} = \frac{\frac{1}{2\pi K_{wL}}}{R_{eq}} \quad \text{(Eq. 13)}$$

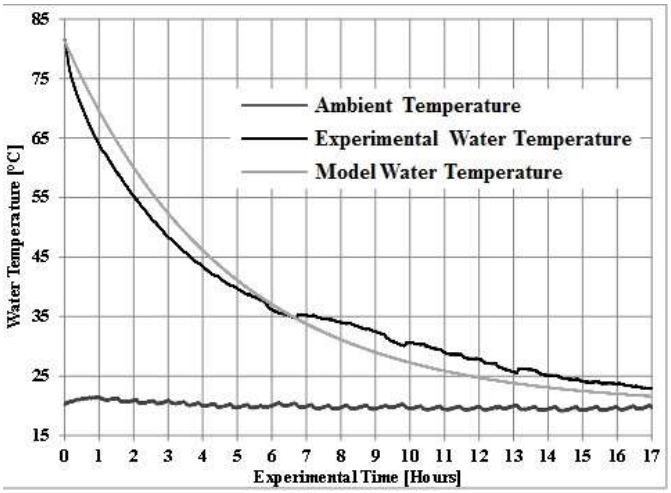

Figure 4. Experimental and Modeled HCE Temperature-Time Histories During Cool-Down.

The Biot number is 0.0012 for this system, meaning the lumped capacitance model, Eq. 14, is a valid thermal performance approximation.

$$T_{s1}(t) = (T_{s1} - T_a) e^{-\frac{t}{C_{sys} R_{tot}}} + T_a \quad \text{(Eq. 14)}$$

To determine an experimental value for thermal resistance presented by the HCE, Eq. 14 was plotted juxtaposed against the experimental data, as shown in Figure 4. The product C_{sys}*R_{tot} was treated as a variable parameter. For each C_{sys}*R_{tot} selected, the standard error of the estimate (SEE) between the model and experiment was calculated. The C_{sys}*R_{tot} parameter was then changed until SEE was minimized, which corresponded to C_{sys}*R_{tot} = 16910 s. Knowing the volume and density of water in the HCE, its thermal mass, C_{sys}, was found to be 7620 J/K; leaving R_{tot} = 2.22 K/W. This resistance, therefore, represents the best value using a lumped capacitance model to approximate the experimentally measured HCE cool-down process.

IV. Discussion

At first inspection, the experimental result, R_{tot} = 2.22 K/W, seems poorly matched to the analytical model, R_{eq} = 0.6459 K/W. However, over 93% of the total heat transfer resistance is represented by the parallel path presented by

R_3 and R_4. Moreover, the exact value of R_3 is highly susceptible to the conductivity of gas in the evacuated annulus between the steel pipe and the glass envelope. The R_3 analysis described above assumed ideal gas behavior in the evacuated space – in other words, thermal conductivity is not a function of pressure. Thus, the k_{air} value used was for air at atmospheric pressure despite the rarified condition in the envelope. While there was no way to directly measure the pressure inside the HCE, air rarified to lower-than-ambient pressure would yield a lower k_{air} value. This reduction in air conductivity with increasing vacuum would increase R_{eq} toward closer agreement with R_{tot}. Given the difficulty in fixing R_3 without breaking open the HCE to directly measure the pressure in the evacuated space, the model-experimental agreement achieved through our approach is surprisingly strong. The experimental and analytical resistance values for the HCE differ by only 3.44 times.

V. Conclusion

A technique was described to experimentally measure the total resistance to heat transfer presented by the HCE of a parabolic trough solar energy collector. After filling the collector with stagnant hot water, it was allowed to cool down over time in an ambient environment at fixed temperature. The resulting temperature-time history was then used to tune the R*C parameter of a lumped capacitance thermal model to minimize the standard error of the estimate between model and experiment. Knowing the thermal mass of water in the system, the resulting best fit value for R can be extracted directly from the experimental data. A value of R_{tot} = 2.22 K/W provided the best match to experimental data for the HCE tested.

In parallel, an analytical resistive network was developed by representing the various HCE heat transfer processes as thermal resistors and collapsing the network into a single equivalent resistor. More than 93% of the equivalent resistor value is represented by the parallel radiation and convection heat transfer paths between the internal steel pipe and outer glass envelope. The large resistance concentrated at this network location is expected because the purpose of this evacuated space is to minimize heat leak from the HCE. A value of R_{eq} = 0.6459 K/W for the HCE we tested was found from the analytical model.

The apparent mismatch between R_{tot} from the experimental method and R_{eq} from the analytical method most likely arises from an incorrect estimate of the thermal conductivity of rarified gas inside the HCE's evacuated space, k_{air}. However, this property cannot be accurately determined without directly measuring the pressure inside the element by opening it to install a pressure gauge; an act which would foul the vacuum. So, the k_{air} value used was that for air at atmospheric pressure acting as an ideal gas. Rarified air has a lower thermal conductivity than air at 1 atmosphere, which would tend to drive R_{eq} closer to R_{tot}.

Acknowledgments

This research was crowd-funded through Microryza. We also acknowledge the National Aeronautics and Space Administration (NASA); Charter Manufacturing; Solar Logic, Inc.; and John Goljenboom Trucking, LLC, for financial and in-kind project support. Undergraduate co-authors working on this project are members of the Milwaukee Undergraduate Researcher Incubator (MURI) at MSOE, an organization which fast-tracks undergraduates into meaningful early research experiences.

References

[1]Traum, M. J., Bohl, G, "Challenging the Dominance of Photovoltaic Energy Though Disruptive Concentrated Solar Power Technologies," Progressive Communities Seminar Series, Office of Sustainability, University of North Texas, Denton, TX, November 9, 2010 (unpublished).

[2]Kennedy, C. E., Price, H. "Progress in development of high-temperature solar-selective coatings," Paper NREL/CP-520–36997, *Proceedings of the 2005 International Solar Energy Conference*, August 6–12, 2005, Orlando, Florida, USA, pp. 749-755.

[3]Bialobrzeski, R. W., "Optimization of a SEGS Solar Field for Cost Effective Power Output," M.S. Thesis, Mechanical Engineering Department, Georgia Institute of Technology, Atlanta, GA, 2007.

[4]Bergman, T. L., Lavine, A. S., Incropera, F. P., DeWitt, D. P., *Introduction to Heat Transfer, 6th Edition*, John Wiley & Sons, Inc., Hoboken, NJ, 2011, pp. 581-582.

[5]Duffie, J. A., Beckman W. A., *Solar Engineering of Thermal Processes, 3rd Edition*, John Wiley & Sons, Inc., Hoboken, NJ, 2006.